Dielectric properties of lead-free ceramics with perovskite structure

J. Kulawik, D. Szwagierczak, S. Nowak

Institute of Electron Technology, Cracow Division, 30-701 Kraków, Zabłocie 39, Poland

Abstract

The aim of the work was searching for new lead-free high permittivity materials of perovskite structure. Four compounds with compositions analogous to relaxor ferroelectrics - $Bi_{1/2}Cu_{1/2}(Fe_{2/3}W_{1/3})O_3$ (BCFW), $Bi_{1/2}Cu_{1/2}(Fe_{1/2}Ta_{1/2})O_3$ (BCFT), $Bi_{1/2}Cu_{1/2}(Zn_{1/3}Nb_{2/3})O_3$ (BCZN), and $Bi_{1/2}Cu_{1/2}(Mg_{1/3}Nb_{2/3})O_3$ (BCMN), in which lead was substituted by bismuth and copper, were synthesized. Phase composition of the synthesized powders was detected by X-ray diffraction analysis. The ceramic pellets were sintered at temperatures 870 - 1050°C. Capacitance and dissipation factor of the specimens were measured in the temperature range from –55 to 400°C at frequencies 10 Hz – 1 MHz. Resistivity of the ceramics was investigated as a function of temperature in the range 20 - 500°C. Microstructure and chemical composition of the samples were studied using scanning electron microscopy and X-ray microanalysis. As a result of the sintering of all synthesized materials dense ceramics were obtained. BCFW, BCFT and BCZN specimens showed a broad maximum in dielectric permittivity versus temperature plots and a distinct dependence of dielectric properties on frequency. The maximum relative permittivity of these materials was very high (30000 - 40000 at 1 kHz). Maxwell-Wagner polarization is supposed to be responsible for these values. The dielectric permittivity for BCMN ceramics was found to be much lower (1000 at 1 kHz). Some maxima in dissipation factor versus temperature plots were also observed, shifting towards higher temperatures with increasing frequency. Relaxation times corresponding to the peak frequencies obeyed well Arrhenius law.

Keywords: dielectric properties (C), perovskites (D), lead-free ceramics (D)

1. Introduction

There is a raising tendency to search for new materials which could become less hazardous for environment alternatives to lead based relaxor ferroelectric compounds, widely used at present in piezoelectric, pyroelectric and capacitor applications. Recently, there can be noticed growing interest in the lead-free piezoelectric and capacitor materials, such as: $Bi_{1/2}Na_{1/2}TiO_3$ [1, 2], $Bi_4Ti_3O_{12}$, $SrBi_4Ti_4O_{15}$ [3, 4] $KNbO_3$ [5], $NaNbO_3$ [6] $CaCu_3Ti_4O_{12}$ [7, 8], $BaFe_{1/2}Nb_{1/2}O_3$ [9].

The subject of this work were compounds of perovskite structure and the compositions similar to those of relaxor ferroelectrics, in which lead has been replaced by bismuth and copper - $Bi_{1/2}Cu_{1/2}(Fe_{2/3}W_{1/3})O_3$ (BCFW), $Bi_{1/2}Cu_{1/2}(Fe_{1/2}Ta_{1/2})O_3$ (BCFT), $Bi_{1/2}Cu_{1/2}(Zn_{1/3}Nb_{2/3})O_3$ (BCZN) and $Bi_{1/2}Cu_{1/2}(Mg_{1/3}Nb_{2/3})O_3$ (BCMN). Bismuth is a good substitute for lead and its insoluble compounds are generally considered to be of low toxicity. The study of the phase composition and microstructure of the developed ceramics as well as determination of their dielectric properties as a function of temperature and frequency seems to be essential for the evaluation of the potential applications of these materials.

2. Experimental procedure

The two step “columbite” and “wolframite” methods developed by Swartz and Shrout [10] were utilized for the synthesis of the compounds with compositions: $Bi_{1/2}Cu_{1/2}(Fe_{2/3}W_{1/3})O_3$ (BCFW), $Bi_{1/2}Cu_{1/2}(Fe_{1/2}Ta_{1/2})O_3$ (BCFT), $Bi_{1/2}Cu_{1/2}(Zn_{1/3}Nb_{2/3})O_3$ (BCZN), and $Bi_{1/2}Cu_{1/2}(Mg_{1/3}Nb_{2/3})O_3$ (BCMN). The oxides of B-site cations (Fe_2O_3 and WO_3, MgO and Nb_2O_5, ZnO and Nb_2O_5, Fe_2O_3 and Ta_2O_5) were prereacted prior to the reaction with A-site cations (Bi_2O_3 and Cu_2O). Addition of 0.5 - 1% of MnO_2 was used in order to enhance resistivity of the materials. In the case of the BCZN synthesis 10 mol % of $BaTiO_3$ was introduced to increase stability of the perovskite structure. The oxides were

weighted in stoichiometric proportions, ball-milled in alcohol, dried and pelletized. The first reaction step was carried out at 950 - 1000°C for 4 h, the second one at 800 - 850°C for 4 h. For example, the course of the synthesis for BCW was the following:

step I $Fe_2O_3 + WO_3 \rightarrow Fe_2WO_6$

step II $4\ Fe_2WO_6 + 3Bi_2O_3 + 3Cu_2O \rightarrow 12\ Bi_{1/2}Cu_{1/2}(Fe_{2/3}W_{1/3})O_3$

The products obtained as a result of the syntheses were milled, mixed with 3% water solution of polyvinyl alcohol, granulated, pressed into discs and sintered for 1 - 2 h in closed crucibles. The sintering temperatures were: 870°C, 1050°C, 940°C and 1000°C for BCFW, BCFT, 0.9BCZN-0.1BT and BCMN, respectively. Phase composition of the sintered samples was detected by a Philips X'Pert X-ray diffractometer.

The values of dielectric permittivity and dissipation factor were determined in the temperature range from -55 to 400°C at frequencies 10 Hz – 1 MHz by the aid of a 7600 LCR QuadTech meter. Dc resistivity of the samples was measured in the temperature range 20 - 500°C using a 6517A Keithley electrometer and a Philips resistance meter.

Microstructure and chemical composition of the sintered samples were studied by means of a Joel scanning electron microscope and a Link Isis X-ray microprobe.

3. Results and discussion

The X-ray diffraction analysis has shown that as a result of the syntheses described above new crystalline products were formed. The obtained patterns did not correspond to any powder diffraction files available in ICDD database.

In the case of all the synthesized materials the sintering process led to the formation of dense samples with a small porosity. Figs. 1 and 2 illustrate the microstructure of BCFT and BCFW ceramics. The size of the grains was not uniform, changing from 1 to 7 μm for BCFW

specimens. Microprobe analysis has also revealed some inhomogeneity in chemical composition.

For the investigated ceramics in the examined temperature range some broad maxima of electrical permittivity (ε_r) were observed related to the relaxation process. These peaks shift towards higher temperatures with increasing frequency. The values of ε_r maximum decrease as frequency is raised. Flattening of the $\varepsilon_r(T)$ relationship occurs both for the low temperature and the high frequency regions. At higher temperatures a subsequent monotonous increase of the dielectric permittivity takes place due to electrical conduction. This behaviour is illustrated in Figs. 3 and 4 for BCFT and BCFW ceramics. BCFW, BCFT and 0.9BCZN-0.1PT specimens show a very high maximum dielectric permittivity – about 30000 – 40000 at 1 kHz. The ε_r maxima are located in the temperature range 70 – 360°C, depending strongly on frequency. The rapid drop in permittivity values begin in the temperature range from –50 to 20°C. The permittivity values for BCMN ceramic at 1 kHz are at the level of 1000, much lower than those for three other materials under investigation.

In the case of dissipation factor versus temperature plots the peaks are observed in a lower temperature range as compared with the ε_r maxima. In Fig. 5 the temperature dependence of dissipation factor for a BCFT sample is presented. Dissipation factor maxima increase and are shifted towards higher temperatures with increasing frequency.

For Debye-type monodispersive dielectric relaxation a maximum of tgδ occurs when the condition $\omega\tau=1$ is fulfilled, where ω is angular frequency ($\omega=2\pi f$) and τ - the relaxation time. In Fig. 6 the logarithm of relaxation time is plotted as a function of 1000/T for BCFW, BCFT and 0.9BCZN-0.1BT ceramics. The linear nature of these plots indicate that the relaxation time τ follows the Arrhenius law:

$$\tau = \tau_0 \exp\frac{E_\tau}{k_B T}$$

where E_τ is the activation energy of dielectric relaxation, k_B – Boltzmann constant, T - temperature.

It was found that the activation energies of dielectric relaxation did not differ significantly for these three materials, ranging from 0.31 to 0.42 eV.

In Fig. 7 the temperature dependencies of conductivity are presented for all the examined materials. The temperature dependence of electrical conductivity σ for the examined samples obeys well the Arrhenius relationship:

$$\sigma = \sigma_0 \exp \frac{E_\sigma}{k_B T}$$

where E_σ is the activation energy of electrical conduction, k_B – Boltzmann constant, T - temperature.

There occur two linear segments of the plots. The steeper slopes, corresponding to activation energies 0.4 - 0.64 eV, are observed at temperatures above 120 - 150°C. The lower and almost the same for all the investigated compositions E_σ values of 0.35 – 0.39 eV were calculated for the temperature range 20 –120°C.

In Fig. 8 the Arrhenius plots for the relaxation time and the dc electrical conductivity determined in the similar temperature range are compared for a 0.9BCZN-0.1BT sample. It can be stated that the slopes of both plots and consequently the relevant activation energies are quite similar (0.41 eV and 0.42 eV). This suggests the contribution of the mobile charge carriers to the dielectric relaxation process.

It seems that the dielectric characteristics observed for $Bi_{1/2}Cu_{1/2}(Fe_{2/3}W_{1/3})O_3$ (BCFW), $Bi_{1/2}Cu_{1/2}(Fe_{1/2}Ta_{1/2})O_3$ (BCFT) and $Bi_{1/2}Cu_{1/2}(Zn_{1/3}Nb_{2/3})O_3$ are close to those reported for some nonferroelectric materials with perovskite structure, such as $CaCu_3Ti_4O_{12}$ [7, 8] and $AFe_{0.5}B_{0.5}O_3$ (A = Ba, Sr, Ca; B = Nb, Ta, Sb) [9]. These compounds exhibit low permittivity at temperatures below the step and a very high and almost independent of temperature

permittivity above this step. Such behaviour has been attributed to the formation of internal barrier capacitor [7] or Maxwell-Wagner polarization arising from electrical inhomogeneity [9]. Similarly, in this work for BCFW, BCFT and BCZN ceramics small values of ε_r (40 - 200) were found at lower temperatures and a rapid increase in dielectric constant occurs at higher temperatures. The observed extremely high values of permittivity at low frequencies (10 and 100 Hz) and inhomogeneous microstructure indicate that Maxwell-Wagner polarization may be responsible for the dielectric behaviour of BCFW, BCFT and BCZN ceramics.

Conclusions

Four compounds with compositions $Bi_{1/2}Cu_{1/2}(Fe_{2/3}W_{1/3})O_3$ (BCFW), $Bi_{1/2}Cu_{1/2}(Fe_{1/2}Ta_{1/2})O_3$ (BCFT), $Bi_{1/2}Cu_{1/2}(Zn_{1/3}Nb_{2/3})O_3$ (BCZN), and $Bi_{1/2}Cu_{1/2}(Mg_{1/3}Nb_{2/3})O_3$ (BCMN) with perovskite structure were synthesized and sintered. BCFW, BCFT and BCZN ceramics showed a very high dielectric constant, a broad maximum in electrical permittivity versus temperature plots and a strong dependence of dielectric properties on frequency. The extremely high values of ε_r at low frequencies are supposed to be attributed to Maxwell-Wagner polarization.

References

1. Chiang, Y. M., Farrey, G. W., Soukhojak, A. N., Lead-free high-strain single-crystal piezoelectrics in the alkaline–bismuth–titanate perovskite family. *Applied Physics Letters* 1998, **73**, [25], 3683-3685
2. Herubut, A. & Safari, A., Processing and Electromechanical Properties of $(Bi_{0.5}Na_{0.5})_{(1-1.5x)}La_xTiO_3$ Ceramics. *J. Am. Ceram. Soc*., 1997, **80**, [11], 2954-58
3. Maeder, M. D., Damjanovic D., Non-Lead Based Piezoelectric Materials. *Piezoelectric Materials in Devices*, edited by N. Setter, Lausanne, Switzerland, 2002
4. Reaney, I. M., Damjanovic, D., Crystal Structure and Domain-wall Contribution to the piezoelectric Properties of Strontium Bismuth Titanate Ceramics. *J. Appl. Phys*., 1996, **80** [7], 4223
5. Sundarakannan, B., Kakimoto, K., Ohsato, H., Frequency and temperature dependent dielectric and conductivity behavior of $KNbO_3$. *J. Appl. Phys.,* 2003, **94,** [8], 5182-5187
6. Raevski, I. P. & Prosandeev, S. A., New Lead Free Perovskites with a Diffuse Phase Transition: $NaNbO_3$ Solid Solutions in *AIP Conf. Proc.*, 2002, **626** [1] 294
7. Sinclair, D. C., Adams, T. B., Morrison, F. D., West, A. R., $CaCu_3Ti_4O_{12}$: One-step internal barrier layer capacitor. *App. Phys. Lett*., 2002, **80**; [12], 2153-2155
8. Lixin Xe, Neaton, J. B., Cohen, M. H., Vanderbilt, D., Homes, C. C., First-principles study of the structure and lattice dielectric response of $CaCu_3Ti_4O_{12}$. *Phys. Rev. B*, 2002, **65**, 214112
9. Raevski, P., Prosandeev, S. A. , Bogatin, A. S., Malitskaya, M. A., Jastrabik L., High dielectric permittivity in $AFe_{1/2}B_{1/2}O_3$ nonferroelectric perovskite ceramics (A=Ba, Sr, Ca; B=Nb, Ta, Sb). *J. Appl. Phys.,* 2003, **93,** [7], 4130
10. Swartz, S. L., Shrout, T. R., Schulze, W. A., Cross, L. E., Dielectric Properties of Lead-Magnesium Niobate Ceramics. *J. Am. Ceram. Soc.,* 1984, **67**, [5], 311

Figure legends

Fig. 1. SEM micrograph of fracture of a $Bi_{1/2}Cu_{1/2}(Fe_{1/2}Ta_{1/2})O_3$ sample

Fig. 2. SEM micrograph of fracture of a $Bi_{1/2}Cu_{1/2}(Fe_{2/3}W_{1/3})O_3$ sample

Fig. 3. Temperature dependence of dielectric permittivity for $Bi_{1/2}Cu_{1/2}(Fe_{1/2}Ta_{1/2})O_3$ ceramic

Fig. 4. Temperature dependence of dielectric permittivity for $Bi_{1/2}Cu_{1/2}(Fe_{2/3}W_{1/3})O_3$ ceramic

Fig. 5. Dissipation factor as a function of temperature for $Bi_{1/2}Cu_{1/2}(Fe_{1/2}Ta_{1/2})O_3$ ceramic

Fig.6. Arrhenius plots of relaxation time for $Bi_{1/2}Cu_{1/2}(Fe_{2/3}W_{1/3})O_3$, $Bi_{1/2}Cu_{1/2}(Fe_{1/2}Ta_{1/2})O_3$ and $0.9Bi_{1/2}Cu_{1/2}(Zn_{1/3}Nb_{2/3})O_3$–0.1 $BaTiO_3$ ceramics

Fig. 7. Temperature dependence of dc conductivity for $Bi_{1/2}Cu_{1/2}(Fe_{2/3}W_{1/3})O_3$ $Bi_{1/2}Cu_{1/2}(Fe_{1/2}Ta_{1/2})O_3$, $0.9Bi_{1/2}Cu_{1/2}(Zn_{1/3}Nb_{2/3})O_3$–0.1 $BaTiO_3$ and $Bi_{1/2}Cu_{1/2}(Mg_{1/3}Nb_{2/3})O_3$ ceramics

Fig. 8. Temperature dependencies of resistivity and relaxation time compared for $0.9Bi_{1/2}Cu_{1/2}(Zn_{1/3}Nb_{2/3})O_3$–0.1 $BaTiO_3$ ceramic

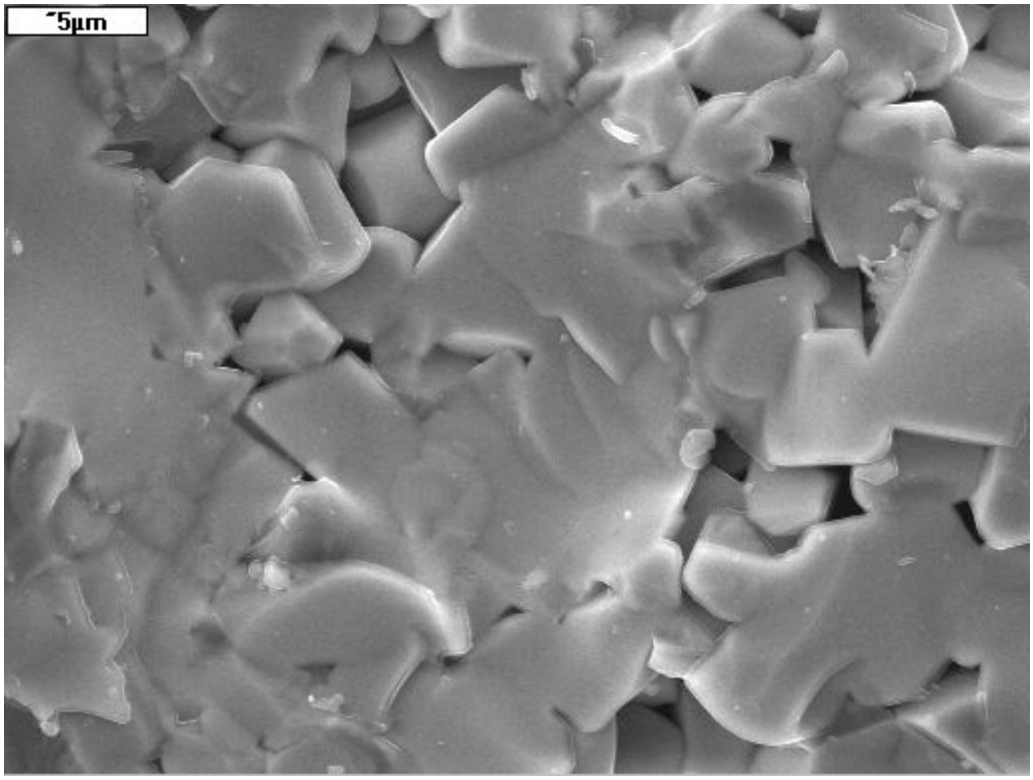

Fig. 1

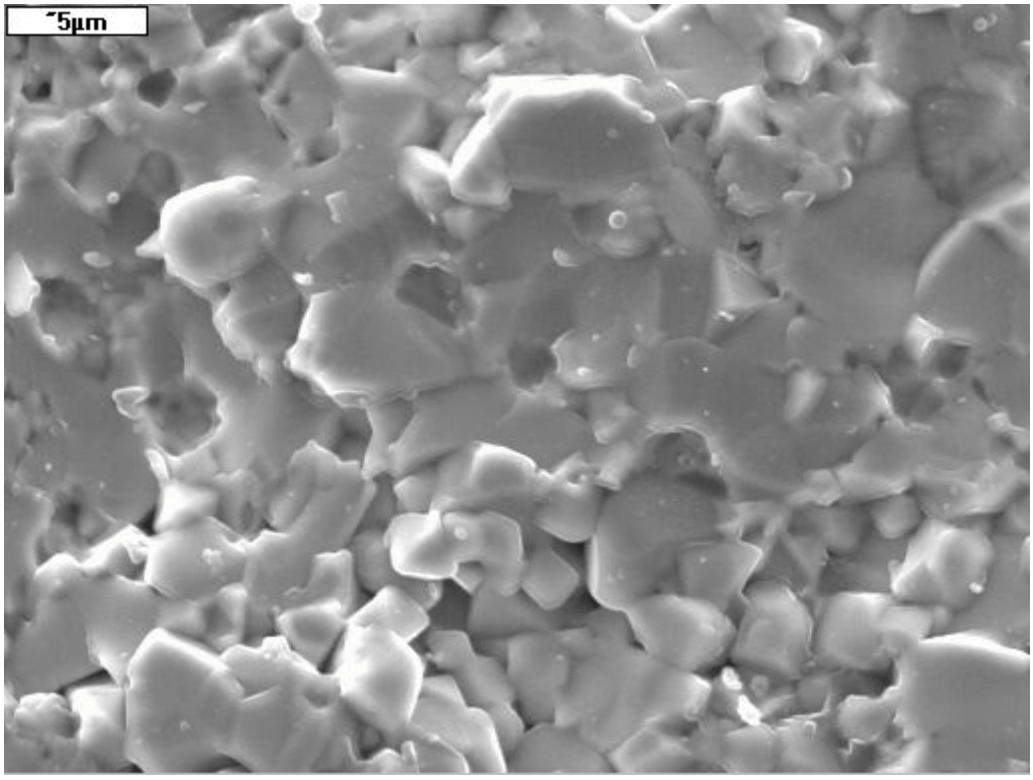

Fig. 2

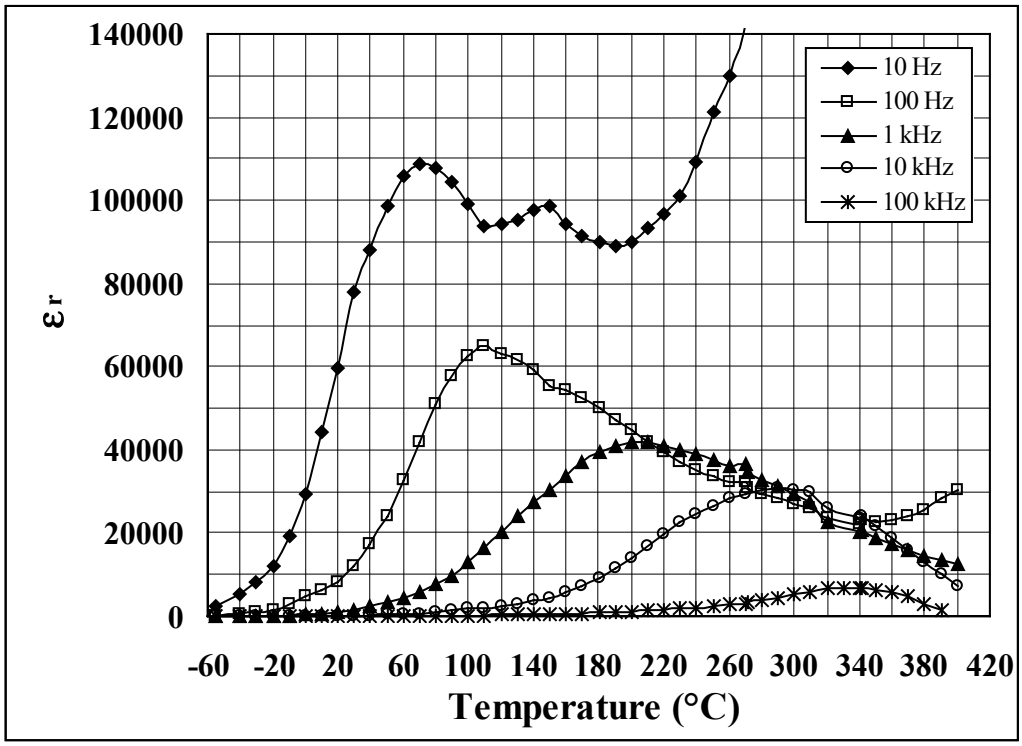
140000
120000
100000
80000
60000
40000
20000
0
εr
10 Hz
100 Hz
1 kHz
10 kHz
100 kHz
-60 -20 20 60 100 140 180 220 260 300 340 380 420
Temperature (°C)

Fig. 3

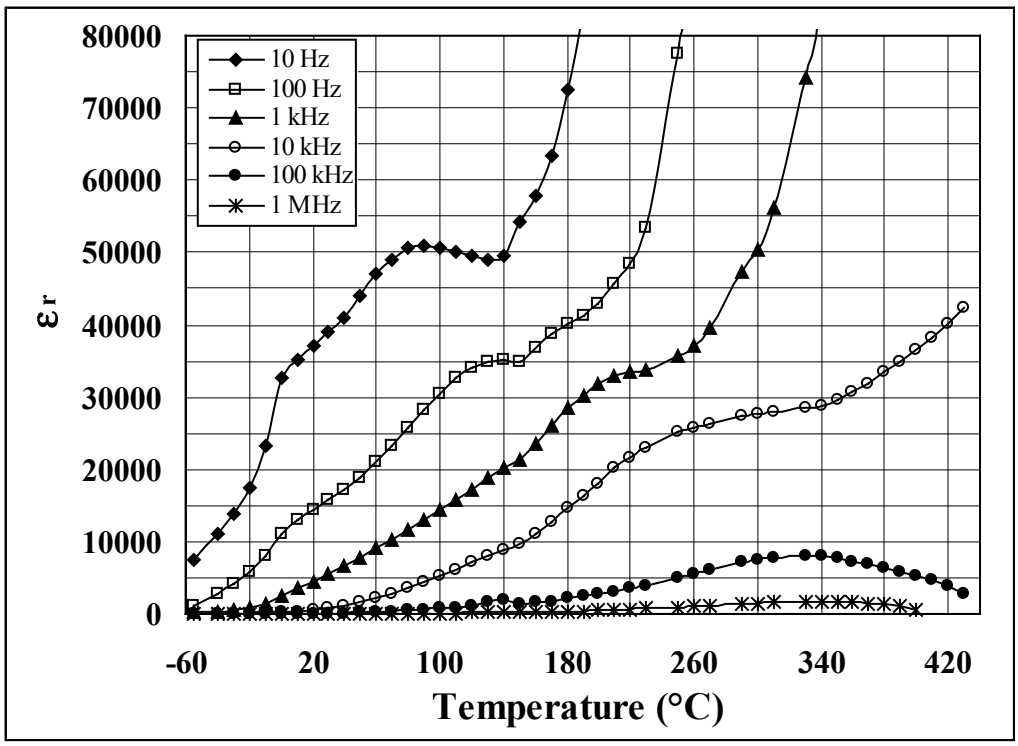
80000
70000
60000
50000
40000
30000
20000
10000
0
εr
10 Hz
100 Hz
1 kHz
10 kHz
100 kHz
1 MHz
-60 20 100 180 260 340 420
Temperature (°C)

Fig. 4

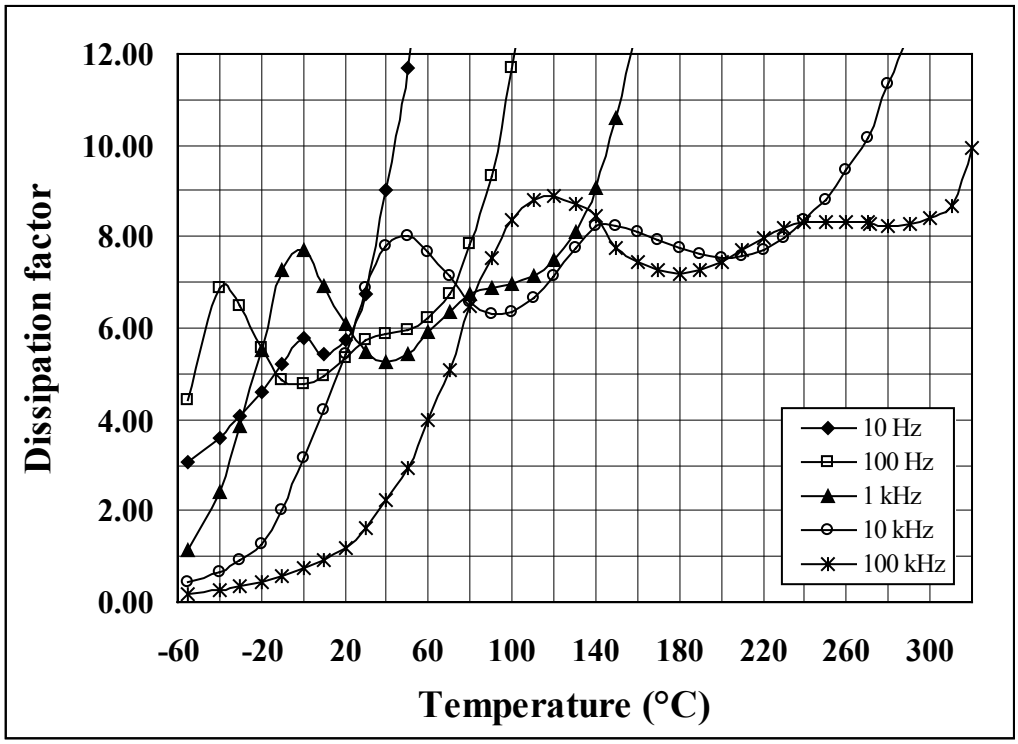
12.00
10.00
8.00
6.00
4.00
2.00
0.00
Dissipation factor
-60
-20
20
60
100
140
180
220
260
300
Temperature (°C)
10 Hz
100 Hz
1 kHz
10 kHz
100 kHz

Fig. 5.

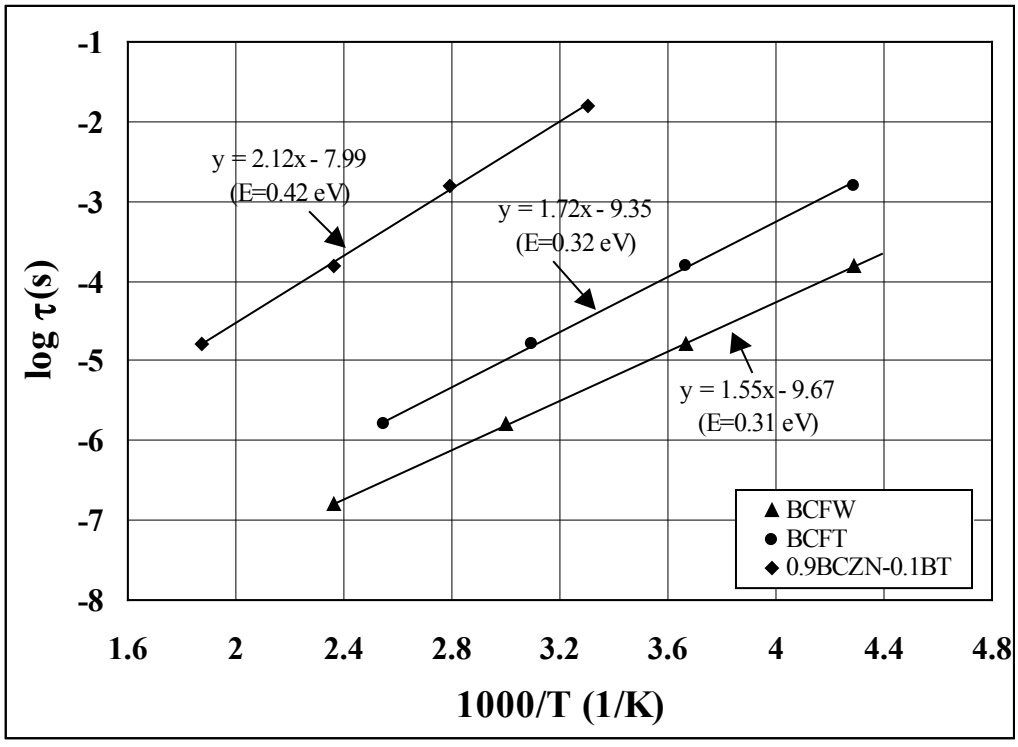
-1
-2
-3
-4
-5
-6
-7
-8
log τ(s)
y = 2.12x - 7.99
(E=0.42 eV)
y = 1.72x - 9.35
(E=0.32 eV)
y = 1.55x - 9.67
(E=0.31 eV)
BCFW
BCFT
0.9BCZN-0.1BT
1.6
2
2.4
2.8
3.2
3.6
4
4.4
4.8
1000/T (1/K)

Fig. 6.

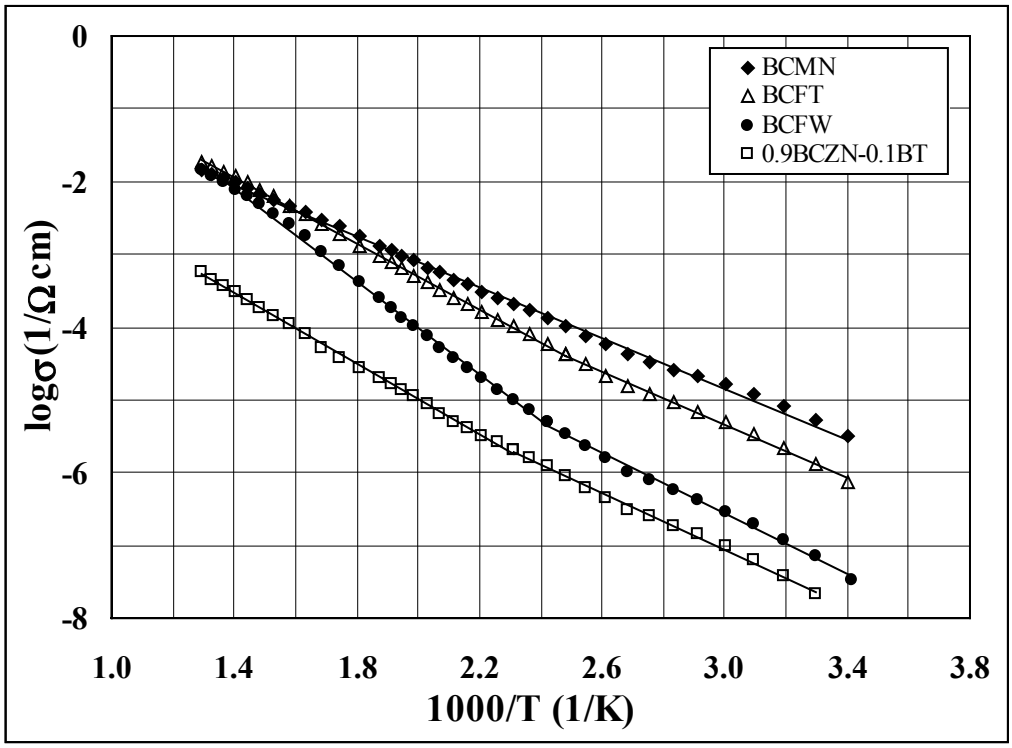
BCMN
BCFT
BCFW
0.9BCZN-0.1BT
logσ(1/Ωcm)
0
-2
-4
-6
-8
1.0
1.4
1.8
2.2
2.6
3.0
3.4
3.8
1000/T (1/K)

Fig. 7

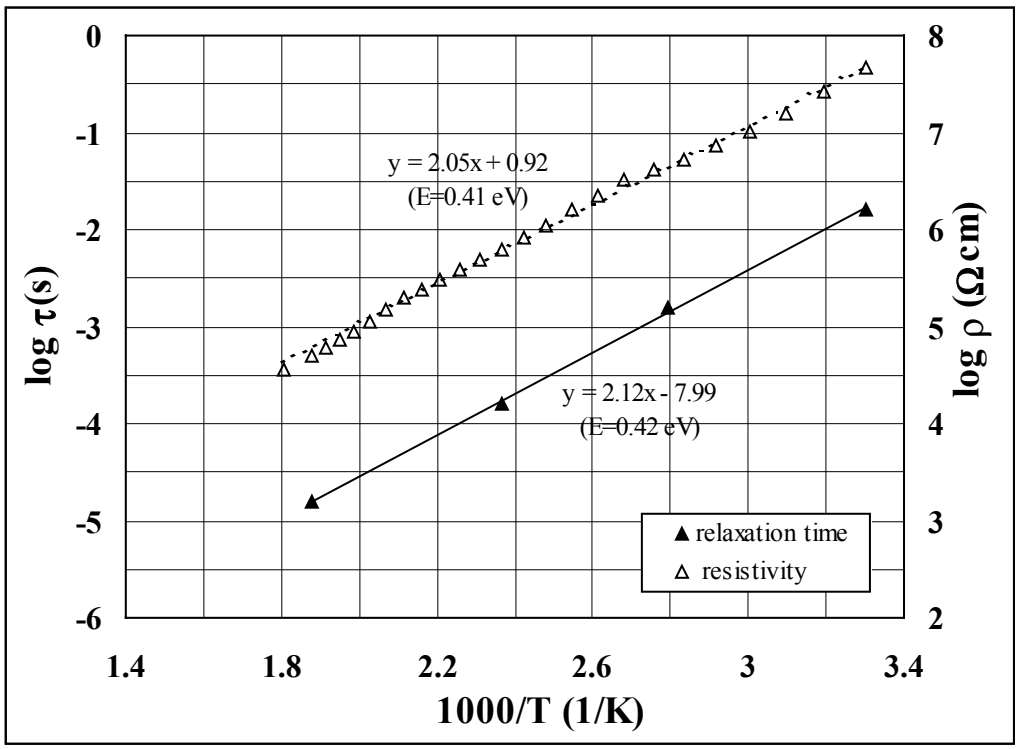
y = 2.05x + 0.92
(E=0.41 eV)
y = 2.12x - 7.99
(E=0.42 eV)
relaxation time
resistivity
log τ(s)
log ρ (Ωcm)
0
-1
-2
-3
-4
-5
-6
8
7
6
5
4
3
2
1.4
1.8
2.2
2.6
3
3.4
1000/T (1/K)

Fig. 8